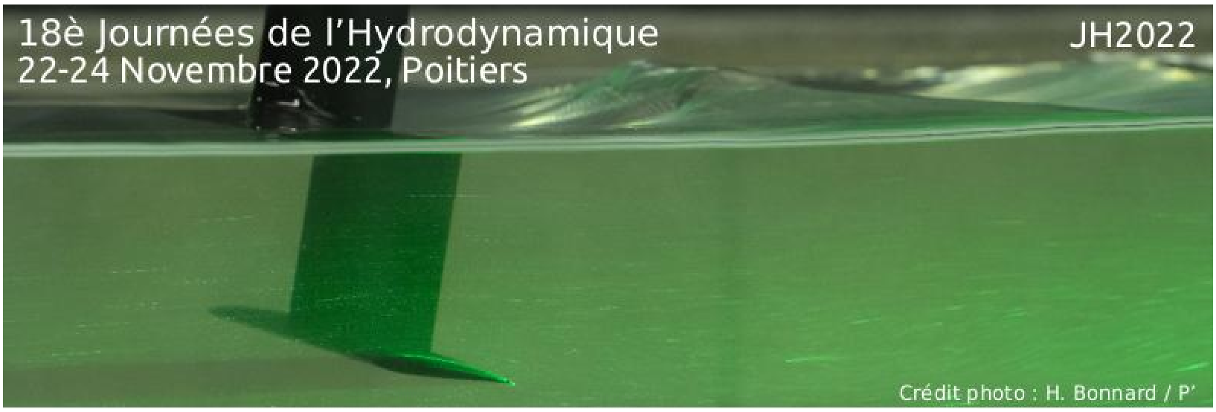

AN EMPIRICAL WAKE MODEL ACCOUNTING FOR VELOCITY DEFICIT AND TURBULENCE INTENSITY IN A SIMPLE TIDAL PARK

K.B. SHARIFF and S.S. GUILLOU

kabir-bashir.shariff@unicaen.fr ; sylvain.guillou@unicaen.fr

Normandie Université, UNICAEN, LUSAC, EA4253, 60 rue Max Pol Fouchet, 50130, Cherbourg-Octeville, France

Résumé

Cette étude présente le développement d'un modèle à bas coût de calcul pour estimer le déficit de vélocité et l'intensité de la turbulence dans le sillage d'une turbine hydrolienne en grandeur réelle. Le modèle proposé est appliqué dans un canal idéal dont les conditions hydrodynamiques sont similaires à celle du Raz Blanchard. Une configuration de ferme pilote de 10 turbines est considérée. Le modèle fournit des résultats raisonnables comparés aux données obtenues avec un modèle numériques plus complet, en particulier dans la région du sillage lointain. Cependant, une variation apparaît dans le résultat du modèle en déficit de vitesse qui peut être attribuée à l'utilisation de la turbulence ambiante de la ferme.

Summary

This study presents a low computational model developed to estimate the velocity deficit and turbulence intensity in the wake of full-scale tidal turbine. The proposed model is applied in an ideal channel with hydrodynamics similar to the Alderney Race consisting of 10 turbines with realistic configuration. The model provides reasonable results compared to the numerical data, especially in the far wake region. However, the appearing variation in the velocity deficit model may be attributed to the use of ambient turbulence on the farm.

I – Introduction

Over the last decade, the tidal energy industry has recorded successful deployment and testing of full-scale Tidal Stream Turbines (TST) at dedicated test sites and commercial

project locations [2]. Commercial-scale tidal energy production requires a cluster network of TST in energetic sites. Recently, the Normandie Région in France has consented to the development of two pilot farm projects in the Alderney Race ; the 11 MW Normandie Hydrolienne and the 17.5 MW Flowatt project [15]. A cluster network of turbine arrays can reduce costs by sharing infrastructure and collective maintenance. As the energetic tidal sites are limited by size, depth, and shipping routes, this results in placing devices close together. However, turbine wake affects downstream turbine performance by decreasing the unit energy production and increasing the turbulence in the flow. This mutual wake interaction can decrease the overall farm efficiency [16].
Experimental investigation of turbine wake at different configurations has been established using porous disc [6] and tidal turbine models [5]. Also, numerical models have been used to investigate the effect of turbine spacing on power production in tidal farms. These studies show higher energy production occurs at a lateral spacing of 2 - 3 D while maximizing the longitudinal spacing [16, 1]. The minimal lateral spacing can accelerate the flow for the downstream turbine while the large longitudinal spacing ensures flow recovery. For this reason, the staggered array produces higher energy than the rectilinear array with the same number of turbines in a particular site [16].
In addition, empirical models have been developed to estimate the wake of single and multiple turbines in a tidal farm [3, 10]. These models are used mainly in commercial tools due to their flexibility and low computational cost. However, these models are largely limited to velocity deficit models as it directly relates to power extraction in the farm.
In this study, we proposed an empirical model for turbulence intensity and the velocity deficit in TST wake. This paper extends the previous work of the authors on modeling the added turbulence of a single turbine [12]. The present study aims to implement the model in a park to investigate the wake interaction in an array of 10 turbines. The paper is part of a project that aim in developing a generic model to optimize electricity production in tidal farm.

II – Numerical model

A 3D numerical model is developed with *OpenFOAM* code with the turbine rotor represented as an actuator disc. The actuator disc method (ADM) applies a uniform thrust force along the disc surface to replicate the pressure jump across the turbine during the energy extraction. Though the ADM underestimates the wake in the initial near wake, it provides acceptable results in the far wake region [7]. The ADM is widely used in wind and tidal farm applications [17]. The uniform thrust force is evaluated as :

$$T = \frac{1}{2}\rho C_T S U_\infty^2 \tag{1}$$

where ρ is the fluid density, S is the rotor cross-sectional area, U_∞ is the upstream velocity and C_T is the thrust coefficient. For multiple turbines, the use of the upstream velocity is debatable due to the wake effect. Therefore, the thrust force is evaluated with the local velocity at the disc location as Eq. (2) :

$$T = \frac{1}{2}\rho \frac{K}{e} U_d^2 \tag{2}$$

where U_d is the velocity at the disc, e is the disc thickness and K is the resistance coefficient which relates to thrust coefficient as $C_T = \frac{K}{\left(1+\frac{1}{4}K\right)^2}$. The thrust force is added as a source term to the momentum equation and solved along with the continuity equation.

A standard $\kappa - \epsilon$ turbulence model is used for Reynold's stress closure. The model is validated in the previous work of the authors [12].
In this study, a full-scale turbine of 20 m diameter (D) is considered in an ideal channel of 50 m depth similar to the Alderney Race in the English Channel. The selection of this rotor size is favored by the Normandie Hydrolienne pilot farm project in the Alderney Race [15]. The numerical domain is 40 D long and 30 D wide. The turbines are located at mid-depth and the first row is 10 D from the inlet to ensure a fully developed flow. The ambient turbulent intensity of 10% is considered which is comparable to the turbulence intensity in the Alderney Race [14]. The inlet condition for the velocity, turbulence kinetic energy, and dissipation is expressed in Eq. (3), a symmetric condition is used at the top and lateral surface, no-slip wall at the bottom and atmospheric pressure at outlet condition.

$$U = \frac{U^*}{\kappa} \ln\left(\frac{z}{z_0}\right), \qquad k = \frac{3}{2} I^2 U^2, \qquad \epsilon = C_\mu^{\frac{3}{4}} \frac{k^{\frac{3}{2}}}{L} \tag{3}$$

where U^* is the frictional velocity of the mean velocity $U = 2.8\ m/s$ similar to the mean velocity in the Alderney Race [14], $\kappa = 0.4$ is the von Karman constant, z is the channel depth, z_0 is the roughness and L is the turbulent length scale defined as the turbine diameter. I is the turbulent intensity, C_μ is the turbulence model constant.

III – Single turbine wake empirical model

III – 1 Turbulence intensity model

Turbulent intensity is the ratio of turbulent velocity fluctuation to the mean velocity expressed. The effective turbulent intensity in the wake of a turbine is expressed as Eq. (4) :

$$\mathrm{I_w} = \left(\mathrm{I_a^2} + \mathrm{I_+^2}\right)^{0.5} \tag{4}$$

where I_w is the total turbulence in the wake, I_a is the ambient turbulence and I_+ is the added turbulence by the rotor. The added turbulence intensity model proposed by the authors [13] is expressed as Eq. (5) :

$$I_+ = a(x/D)^{-b} \qquad \begin{cases} a = 0.16 C_T^{4.83} + 0.179 \\ b = 0.68 I_a + 0.472 \end{cases} \tag{5}$$

The added turbulence model is largely influenced by the turbine rather than the ambient turbulence [13]. The turbulence intensity in the channel is reconstructed according to Eq. (4).

III – 2 Velocity deficit wake radius

The classical theory of turbulence shows the far wake behind a disc is axis-symmetric and self-similar in a free shear flow. The lateral wake profile shown in Figure 1a is approximately Gaussian as reported in the wake of a disc [9]. Using the Full-Width Half Maximum (FWHM) value of the standard Gaussian function, the half radius $r_{1/2}$ is evaluated as $\sqrt{2 \ln 2}\sigma$ (σ is the standard deviation). The wake radius is estimated at 3σ as shown in the shaded region in Figure 1a. The wake radius is reported to be dependent on turbulent intensity [3, 13]. The velocity deficit wake radius is expressed in Eq. (6) is shown in Figure 1b.

$$r_w = c\left(\frac{X - X_0}{D}\right)^d \tag{6}$$
$$c = 2.36 + 4.585 I_a, \quad d = 0.347$$

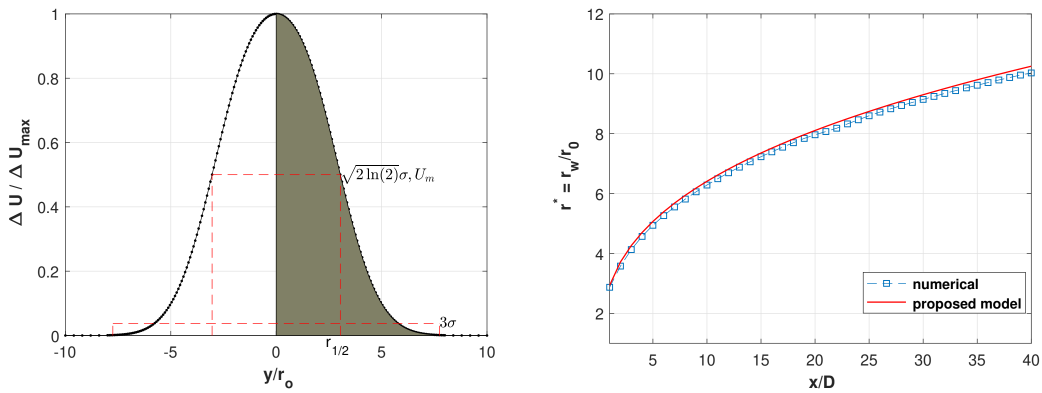

(a) Normalized lateral velocity at 10 D

(b) Normalized wake radius

FIGURE 1 – Evaluation of the velocity deficit radius at 10% ambient turbulence.

III – 3 Velocity deficit model

The velocity deficit is the sum of the stream function and the shape function. To estimate the centerline wake velocity of the tidal turbine, the wake radius model is substituted in the Jensen model presented in Eq. (8). The top-hat shape profile of the Jensen model estimates the average velocity in the wake, while the numerical data provides the minimum wake velocity in the form of a Gaussian profile, as shown in Figure 1a. Assuming the velocity deficit in a lateral plane is Gaussian shape, Lo Brutto et al. [3] proposed a relation for maximum velocity deficit for the Jensen model as Eq. (7) :

$$\Delta U_{\text{def ,max}} = \Delta U_{\text{def , aver}} \left(\frac{r_w}{\sigma}\right)^2 \tag{7}$$

where $\sigma = r_w/2.58$ is the standard deviation. The maximum velocity deficit $\Delta U_{def,max}$ henceforth ΔU_{def} can now be compared with the minimum velocity along the centreline in numerical data. In the present model we propose to use directly a Gaussian model and then estimating directly the velocity deficit in all position in the wake without using a correction coefficient. The velocity deficit is then expressed as Eq.(8) :

$$\frac{\Delta U}{U_\infty} = \left[\frac{\left(1 - \sqrt{1 - C_T}\right)}{\left(\frac{r_w}{r_0}\right)^2}\right] \times \exp\left(-\frac{(y_0 - y)^2 + (z_0 - z)^2)}{r_w^2}\right) \tag{8}$$

where C_T is the thrust coefficient, r_w is the wake radius downstream, σ is the standard deviation coefficient. The exponential function provides the Gaussian shape profile along the lateral plane. The contribution of the model in this study is the inclusion of effective turbulence. The proposed velocity deficit model is compared with the tidal turbine experiment of Mycek et al. [4] as shown in Figure 2. The model is in good agreement with experimental data in the far wake region. However, the model is less accurate in the near wake as a limitation of the ADM.

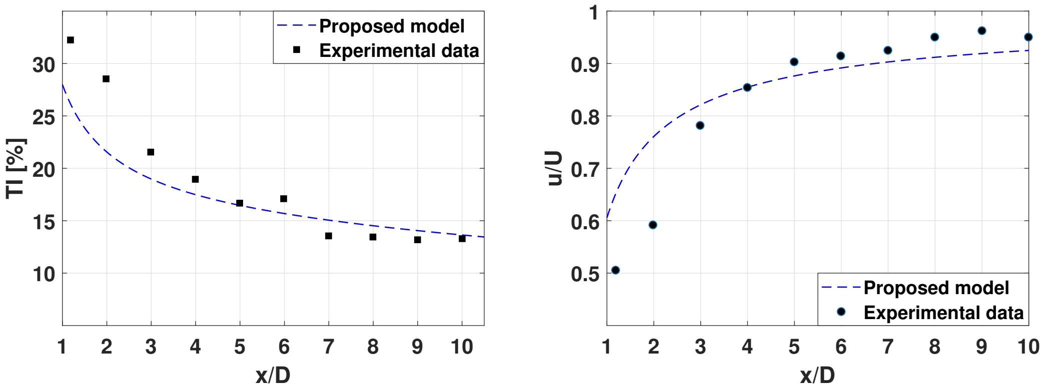

FIGURE 2 – Comparison of the proposed velocity deficit model with tidal turbine experimental data.

IV – Wake interaction

The wake of the upstream turbine affects the energy output of the downstream turbine. To estimate the turbine-wake interaction, several superposition methods are proposed in the literature [8, 11]. In this study, the Squared Sum Method (SSM) is used to estimate the wake interaction. SSM sum the kinetic energy deficit and turbulence energy of turbines ij interacting with turbine j to estimate the interaction effect on the velocity deficit and turbulent intensity. The wake interaction for the turbine in a park for added turbulence and the velocity deficit is expressed as Eq. (9) :

$$
\begin{aligned}
I_w &= I_{amb}^2 + I_{+,j}^2 \\
I_{+,j}^2 &= \sum_{ij=1}^{n} \left(a \left(\frac{x_{ij} - x_i}{D} \right)^{-b} \right)^2 \frac{A_{overlap}}{A_0} \\
\left(1 - \frac{u_j}{U}\right)^2 &= \sum_{ij=1}^{n} \left(1 - \frac{u_{ij}}{U}\right)^2 \frac{A_{overlap}}{A_0}
\end{aligned}
\tag{9}
$$

where $A_{overlap}$ is the overlap area between the expanded wake area A_w of the upstream turbine and the rotor swept area of the downstream rotor A_0. Figure 3 illustrates three scenarios of the wake interaction ; no interaction, full inclusion, and partial interaction. The intersection area is calculated as follows :

$$
A_{overlap} = \begin{cases} 0, & if \quad r_w + r_0 \leq y \\ A_0, & if \quad r_w - r_0 \geq y \\ A_{partial}, & otherwise \end{cases} \tag{10}
$$

where r_w and r_0 are the radius of the wake and turbine respectively, y is the lateral distance between the turbines, and $A_{partial}$ is the intersecting area between the wake area A_w and the rotor swept area A_0 as shown in Figure 4. The wake intersection area $A_{partial}$ is calculated by [8] as Eq. (11) :

$$
A_{overlap} = r_w^2 \left(\theta_w - \frac{\sin(2\theta_w)}{2} \right) + r_0^2 \left(\theta_r - \frac{\sin(2\theta_r)}{2} \right) \tag{11}
$$

where θ_w and θ_0 are the angles of the wake intersection arc and rotor intersection arc respectively and can be respectively expressed as follows :

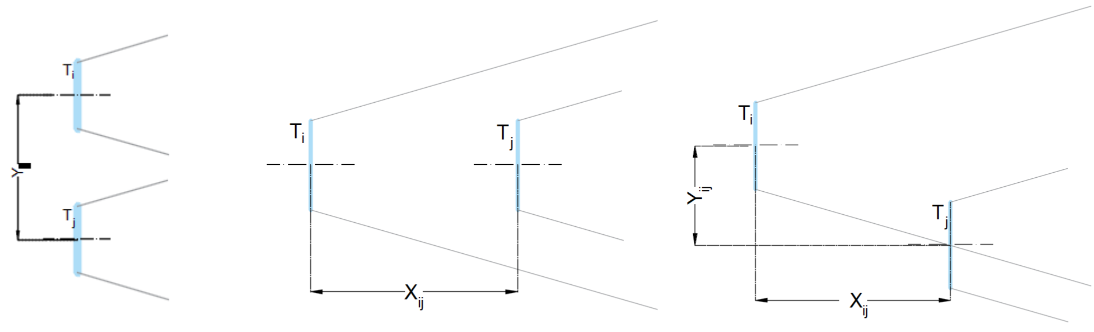

FIGURE 3 – Schematic of turbine-wake interaction ; (a) no interaction (b) fully immersed and (c) partially immersed in the wake of the upstream turbine.

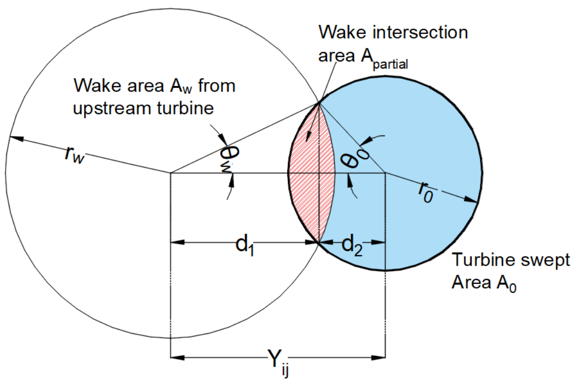

FIGURE 4 – Partial wake area between a wake effect from the upstream turbine and downstream rotor.

$$\theta_w = \cos^{-1}\left(\frac{r_w^2 + y^2 - r_0^2}{2yr_w}\right), \qquad \theta_r = \cos^{-1}\left(\frac{r_w^2 - y^2 - r_0^2}{2yr_0}\right) \tag{12}$$

IV – 1 Tidal array configuration

Tidal turbine park consisting of 10 turbines positioned in a staggered array as shown in Figure 5. The longitudinal and lateral spacing between turbine rows are $7D$ and $3D$ respectively. These arbitrary values have been chosen to reproduce reasonable turbine spacing that may be implemented in a real situation. The ambient turbulence intensity in the park is 10%, and a thrust coefficient of $C_T = 0.89$. The staggered array allows sufficient recovery of the ambient condition of the flow due to sufficient longitudinal spacing between turbines.

The turbines in the first row T_1, T_2, and T_3 detect the unperturbed upstream velocity as there is no prior turbine interaction. The turbines downstream (*row* 2 and *row* 3) are affected by the wake of the upstream turbines. The velocity and turbulence intensity contour along the lateral plane are presented in Figure 6. A zone of increased pressure is observed in the numerical domain (Fig. 6a) as in the actuator disc theory. The empirical model effectively accounts for the wake interaction for both the normalized velocity and the turbulence intensity.

Figure 7 compares the centreline normalized velocity and the turbulence intensity between

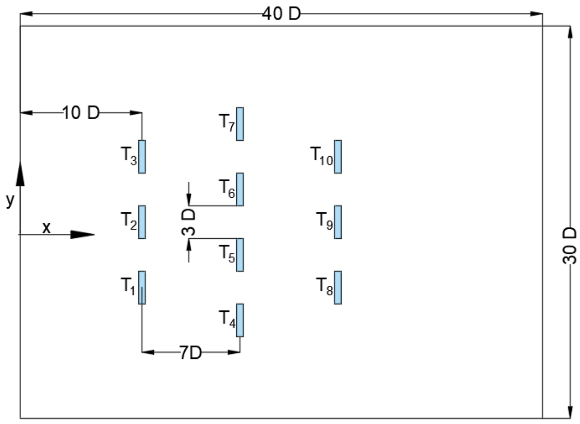

FIGURE 5 – Illustration of the turbine distribution in a staggered array.

the numerical and empirical model with acceptable results. The empirical is valid from $1D$ downstream, below this limit, the model assumes a hyperbolic growth as $\left(\frac{x_{ij}-x_i}{D}\right) \rightarrow 0$. This region corresponds to the nacelle and tower where the wake begins to develop. The variation in the normalized velocity may be due to the use of ambient turbulence in the flow. The turbulence upstream of the first row is ambient turbulence I_a in the flow as no wake effect is induced. However, the turbulence behind a turbine is modified due to the extraction of kinetic energy in the flow. The use of ambient turbulence may be the source of variation as the turbulence in the farm increases dues to turbine-wake interaction. Therefore the use of effective turbulence integrating the effect of the mean added turbulence intensity may improve the model.

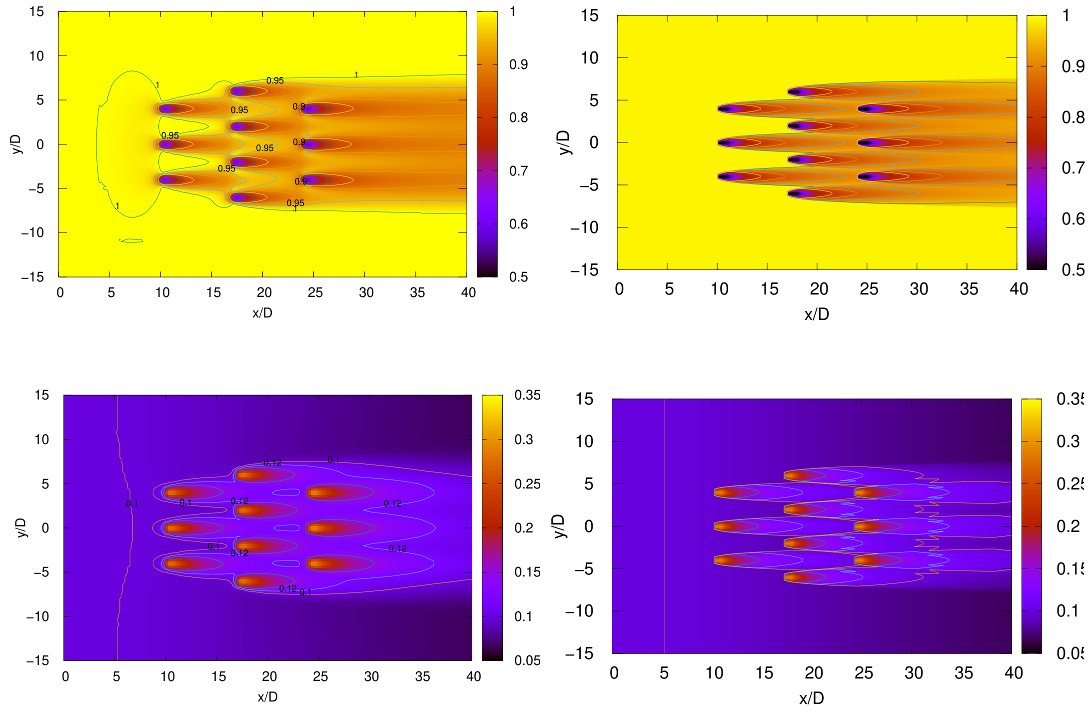

(a) (b)

FIGURE 6 – Numerical (a) and empirical (b) contour showing the normalized velocity (top) and the turbulence intensity (bottom) along the lateral plane.

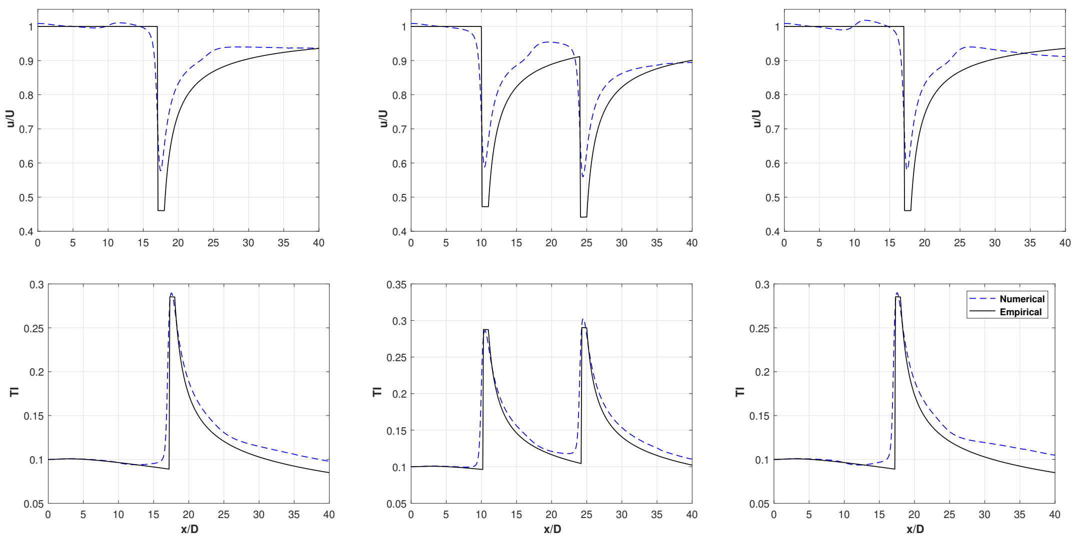

(a) (b) (c)

FIGURE 7 – Comparison of numerical and proposed normalized velocity (top) and turbulence intensity (bottom) of turbines (a) T_7 and T_4, (b) T_1, T_8 and T_2, T_9 and T_3, T_{10}

V – Conclusion

A new empirical model is proposed to predict the velocity deficit and turbulence intensity in the wake of tidal turbine. The following conclusion are obtained :

- The proposed model validated with experimental data of isolated turbine [4] provides acceptable results especially in the far wake.
- The superposition of Square Sum Method (SSM) account for the interaction of upstream turbine.
- The application in a farm provides acceptable results for the velocity deficit and turbulence intensity along the lateral plane.
- The proposed model provides acceptable hydrodynamics along the lateral profile.

To improve the empirical model, the effective turbulence should be considered in the velocity deficit to integrate the effect of mean added turbulent intensity.

Acknowledgement

The work is part of PhD thesis of K. B. Shariff funded by the Region Normandie and the Communauté d'Agglomération du Cotentin, France under the HYDROFARMOD project. S. S. Guillou acknowledges the Interreg VA France (Channel) England Programme, which funds the TIGER project and the Conseil Départemental de la Manche for providing fundings.

Références

[1] G. Bai, J. Li, P. Fan, and G. Li. Numerical investigations of the effects of different arrays on power extractions of horizontal axis tidal current turbines. *Renewable Energy*, 53 :180–186, 2013.

[2] EMEC. Tidal clients : EMEC : European Marine Energy Centre. `https://www.emec.org.uk/about-us/our-tidal-clients/`, 2022.

[3] O. A. Lo Brutto, V. T. Nguyen, S. S. Guillou, J. Thiébot, and H. Gualous. Tidal farm analysis using an analytical model for the flow velocity prediction in the wake of a tidal turbine with small diameter to depth ratio. *Renewable Energy*, 99 :347–359, Dec. 2016.

[4] P. Mycek, B. Gaurier, G. Germain, G. Pinon, and E. Rivoalen. Experimental study of the turbulence intensity effects on marine current turbines behaviour. Part I : One single turbine. *Renewable Energy*, 66 :729–746, June 2014.

[5] P. Mycek, B. Gaurier, G. Germain, G. Pinon, and E. Rivoalen. Experimental study of the turbulence intensity effects on marine current turbines behaviour. Part II : Two interacting turbines. *Renewable Energy*, 68 :876–892, Aug. 2014.

[6] L. Myers and A. Bahaj. An experimental investigation simulating flow effects in first generation marine current energy converter arrays. *Renewable Energy*, 37(1) :28–36, 2012.

[7] V. T. Nguyen, S. S. Guillou, J. Thiébot, and A. Santa Cruz. Modelling turbulence with an Actuator Disk representing a tidal turbine. *Renewable Energy*, 97 :625–635, Nov. 2016.

[8] S. Pookpunt and W. Ongsakul. Optimal placement of wind turbines within wind farm using binary particle swarm optimization with time-varying acceleration coefficients. *Renewable energy*, 55 :266–276, 2013.

[9] S. B. Pope. *Turbulent Flows*. Cambridge University Press, Aug. 2000.

[10] P. Pyakurel, W. Tian, J. H. VanZwieten, and M. Dhanak. Characterization of the mean flow field in the far wake region behind ocean current turbines. *Journal of Ocean Engineering and Marine Energy*, 3(2) :113–123, 2017.

[11] G.-W. Qian and T. Ishihara. Wind farm power maximization through wake steering with a new multiple wake model for prediction of turbulence intensity. *Energy*, 220 :119680, 2021.

[12] K. B. Shariff and S. S. Guillou. Developing an empirical model for added turbulence in a wake of tidal turbine. In *25 ème Congrès Français de Mécanique*, 2022.

[13] K. B. Shariff and S. S. Guillou. An empirical model accounting for added turbulence in the wake of a full-scale turbine in realistic tidal stream conditions. *Applied Ocean Research*, 128 :103329, 2022.

[14] M. Thiébaut, J.-F. Filipot, C. Maisondieu, G. Damblans, C. Jochum, L. F. Kilcher, and S. Guillou. Characterization of the vertical evolution of the three-dimensional turbulence for fatigue design of tidal turbines. *Philosophical Transactions of the Royal Society A : Mathematical, Physical and Engineering Sciences*, 378(2178) :20190495, Aug. 2020.

[15] TIGER-intereg. Le Raz Blanchard demonstration site. `https://interregtiger.com/expanding-the-marine-energy-market/development-sites-and-procurement/le-raz-blanchard/`, 2022.

[16] S. R. Turnock, A. B. Phillips, J. Banks, and R. Nicholls-Lee. Modelling tidal current turbine wakes using a coupled rans-bemt approach as a tool for analysing power capture of arrays of turbines. *Ocean Engineering*, 38(11-12) :1300–1307, 2011.

[17] Y. Zhang, E. Fernandez-Rodriguez, J. Zheng, Y. Zheng, J. Zhang, H. Gu, W. Zang, and X. Lin. A Review on Numerical Development of Tidal Stream Turbine Performance and Wake Prediction. *IEEE Access*, 8 :79325–79337, 2020.